Large homogeneous mono-/bi-layer graphene on 6HSiC(0001) and buffer layer elimination

C Virojanadara, R Yakimova, a A Zakharov, L I Johansson

Large homogeneous mono-/bi- layer graphene on 6H-SiC(0001) and buffer layer elimination.

C. Virojanadara[1], R. Yakimova[1], A. A. Zakharov[2] and L. I. Johansson[1]

[1]Department of Physics, Chemistry and Biology, Linköping University, S-581 83, Linköping, Sweden

[2]Maxlab, Lund University, S-22100, Lund, Sweden

Email: chavi@ifm.liu.se

Abstract. In this paper we discuss and review results of recent studies of epitaxial growth of graphene on silicon carbide. The presentation is focused on high quality, large and uniform layer graphene growth on the SiC(0001) surface and results of using different growth techniques and parameters are compared. This is an important subject because access to high quality graphene sheets on a suitable substrate plays a crucial role for future electronics applications involving patterning. Different techniques used to characterize the graphene grown are summarized. We moreover show that atomic hydrogen exposures can covert a monolayer graphene sample on SiC(0001) to bi-layer graphene without the carbon buffer layer. Thus, a new process to prepare large, homogeneous stable bi-layer graphene sheets on SiC(0001) is presented. The process is shown to be reversible and should be very attractive for various applications, including hydrogen storage.

Keywords

Graphene, epitaxial graphene, SiC, hydrogenation, hydrogen, homogeneous, STM, LEEM, LEED, PES, ARPES

1. Introduction

The potential of graphene, a single layer of carbon arranged in a honeycomb lattice, for advanced nanoelectronics application has been amply demonstrated [1-5]. Its peculiar electronic structure in which charge carriers mimic mass less relativistic particles [6-9] has been verified experimentally. The physical structure of graphene is also fascinating as it behaves like a 2D crystal in which electrons travel up to µm distances without scattering. This makes it superior for transport properties and the material itself is very robust, highly elastic and chemically inert offering a high potential for technological applications. However, for a large scale integration of graphene-based nanoelectronics, access to high-quality graphene sheets on a suitable substrate plays an important role.

Thanks to the SiC composition it is possible to heat a SiC crystal up to elevated temperatures to sublimate the Si atoms and leave a single or few layers of graphene on top of the substrate [10-12]. It is also remarkable that the mono- or multilayer graphene films grown on SiC show electronic properties similar to an isolated graphene sheet [6-8]. These layers typically have metal character with thickness-dependent properties but also the lateral extent is important [8]. Silicon carbide (SiC) is also a good candidate as substrate since it is a robust wide band gap semiconductor and has a superior range of properties from inert to biocompatible and is excellently suited for high temperature and high power applications. For future nanoelectronics applications involving patterning access to homogeneous large area graphene layers on SiC substrates is crucial.

Earlier studies have mainly concentrated on either mechanically exfoliated graphene or on graphene grown on surfaces of SiC by high temperature annealing in vacuum. The former method leads to small isolated, high quality crystals, as the graphene flake illustrated in Fig. 1(a) [4], but is known to be delicate and time consuming. The latter method yields small grains and inhomogeneous graphene layers [13-16], as illustrated in Fig. 1(b)) for the SiC(0001) surface [13]. On the C-terminated SiC(000-1) surface larger grains but multilayer films with an azimuthal disorder between the different layers are typically obtained [14, 17]. Since SiC is an excellent substrate for graphene based electronic devices further efforts [18-23] with the aim to achieve large area graphene with a uniform thickness were recently carried out. These efforts involved growth of the graphene in an ambient gas and were quite successful, since they proved it possible to prepare large and homogenous areas of single layer graphene on the SiC(0001) surface. This review is focused on these efforts and comparisons with earlier findings. In section 2 we briefly describe the different characterization methods utilized. In section 3 different alternatives for epitaxial graphene growth on the SiC(0001) surface are presented and discussed. The focus of section 4 is atomic scale studies of large and homogenous monolayer graphene samples. Last but not least, results from hydrogenation of monolayer graphene on SiC and the ability to improve the graphene/SiC interface are presented in section 5. Agreements and discrepancies obtained between different research groups are also discussed.

2. Measurement techniques

The experimental techniques used to study graphene samples are briefly described in this section. Low energy electron microscope (LEEM), photoelectron spectroscopy (PES) including μ-PES, low energy electron diffraction (LEED) including μ-LEED, angle-resolved photoelectron spectroscopy (ARPES) and scanning tunneling microscopy (STM) were utilized to investigate the morphology, thickness, electronic and atomic structure of the graphene samples grown. Most of our studies were performed at beamlines I311 and I4 at the MAX synchrotron radiation laboratory. The surface atomic structure investigations were, however, carried out at our home laboratory using an Omicron variable temperature STM and tunneling currents of 0.1-0.2 nA using a W tip at room temperature.

The most practical way to investigate the morphology and thickness of graphene samples grown on a SiC substrate is to use LEEM. The LEEM image reveals the homogeneity of the sample prepared and the electron reflectivity measured versus kinetic energy of the incident electron beam allows a direct determination of the number of graphene layers [15, 18] obtained, as demonstrated in Fig. 2. Since LEEM also allows electron diffraction patterns to be collected from small specific areas (μ-LEED) such images are included in Fig. 2. The LEEM image in Fig. 2(a) is an example of uneven growth of graphene layers, since the image shows four distinctly different areas, marked (1)-(4). The electron reflectivity curves collected from these four areas, versus the incident electron beam energy, are displayed in Fig. 2(b). The number of local minima (dips) in the reflectivity curve represents the number of graphene layers [15] and it is clear that the areas do correspond to 1-4 layers of graphene, respectively. The μ-LEED images collected from

these four areas, shown as insets in Fig. 2(a), also show distinct differences in the diffraction pattern. Quite a number of buffer layer spots around the graphene spot (the center/middle spot) are clearly visible for the monolayer graphene, while only six spots around the center can be observed for the bi-layer graphene. These six spots are barely visible from areas with three layers and not possible to detect when the number of layers is larger than three.

The thickness of a graphene sample can also be estimated from recorded C1s PES spectra. For graphene on SiC the C1s spectrum typically consists of three components, i.e. bulk SiC, graphene (G) and the buffer layer (B), located at binding energies of 283.4, 284.4, and 284.9 eV, respectively. Micro and conventional PES spectra recorded from different samples for which the thickness had been determined using LEEM are displayed in Fig. 3(a)-(b). The intensity ratios extracted from these spectra are given in Table 1 and are found to give a fairly good estimation of the number of the graphene layers. It is worth mentioning that the signal was averaged over an area of ca. $1\mu m^2$ for the micro-PES and ca. 0.5 mm^2 for the conventional PES and that the latter were collected at a considerably higher-energy resolution. The ratios obtained from both methods are seen to be quite similar, especially the *G/B* ratio and for a thickness of 1 ML and larger. This way of estimating the thickness can be used as a guideline for *in situ* graphene preparation.

The number of graphene layers obtained from a sample can also be determined using ARPES. From the dispersion and number of the π-bands around the K and Dirac points one can determine directly [6] if the number of layers is 1, 2, 3 or 4. This method do as

the conventional core level PES method mentioned above integrate the signal over an appreciable area and do not provide direct information about the homogeneity of a sample.

3. Graphene growth

3.1 *Ex situ* growth

For the successful development of graphene-based electronic devices the availability of homogeneous large area graphene samples is a crucial factor. However, to prepare uniform wafer size graphene was not a simple task, which the earlier results for graphene growth on the SiC(0001) surface by *in situ* heating [13-16] showed. Small flakes and an inhomogeneous graphene thickness were typically obtained, as illustrated in Fig. 1(b). A refined growth method was clearly needed and a similar idea was actually applied by three different groups at about the same time [18-20]. The idea was to do the growth in an ambient gas, thereby preventing a too fast sublimation of the Si from the substrate and at the same time allowing a higher growth temperature to be used.

We used [18] an inductively heated furnace and carried out the growth under highly isothermal conditions at a temperature of 2000°C and at an ambient argon pressure of 1 atm. Emtsev *et al* [19] also used argon at a similar pressure as the ambient gas but used a growth temperature of 1650°C. Tromp *et al* [20] instead used disilane as the ambient gas and investigated growth temperatures from 800 to 1300°C in an external background Si vapor at a pressure from 10^{-8} to 10^{-6} torr. The presentation below is focused on our results

but includes a comparison to the findings of the other groups. An explanation why growth in an ambient gas and at a higher temperature results in much larger and homogenous graphene samples is provided in the following section, 3.2.

Our first attempt to prepare epitaxial monolayer graphene was made using a 6H-SiC(0001) substrate, having a mis-orientation of within 0.25° [18] from nominally on-axis wafer. The attempt was successful since a homogeneous single domain graphene layer was obtained on large parts of the sample, as displayed in Fig. 4(a). Some areas, however, consisted of two different domains, as shown in Fig. 4(b). It should be noted that the field of view (FOV) is 20 μm in Fig. 4(a) and 50 μm in Fig. 4(b). The number of layers was determined from the collected electron reflectivity curves, as described in section 2. The curves showed only one dip, at an electron energy around 3 eV, which confirmed that the two different domains both corresponded to a single layer of graphene. The origin of the domains is below suggested to originate from interactions between the graphene layer and the buffer layer underneath. Defects on the substrate surface were found to have a dramatic effect on the graphene film formed, as illustrated in Fig. 4(c). The deep scratch appears to draw a line between an area of homogeneous monolayer graphene and areas with a few layers of graphene plus some mixture of domains. The picture illustrates that the density of defects have to be minimized in order to maximize the homogeneity of the graphene formed. A typical LEEM image from this *ex situ* prepared sample at a FOV of 50 μm is shown in Fig. 4(d). The dark stripes show where growth of a second graphene layer has occurred while the bright areas correspond to growth of one single graphene layer.

From the above results, we realized that the surface of the SiC substrate has to be well prepared with few defects in order to achieve an as large and uniform graphene layer as possible. The base pressure within the growth furnace was therefore improved to provide a cleaner surface condition before the temperature was ramped up and the Ar ambient was let in. This resulted in significant improvements of the morphology of the graphene [21], as demonstrated by the LEEM image in Fig. 5(a) at a FOV of 25 μm. The substrate used was cut from the same wafer as the one used above in Fig. 4. The image shows that straighter terraces with a more homogeneous single layer of graphene were obtained. That a better uniformity of domains was also achieved is shown by the LEEM image in Fig. 5(b). For comparison results obtained by Emtsev *et al* [19] using a growth temperature of 1650°C and an argon ambient of 1 atm are illustrated by the LEEM image at a FOV of 15 μm in Fig. 5(c). The bright stripes represent areas where monolayer graphene has formed while the narrower darker stripes contain contributions from two and three layers of graphene.

Substrates cut from a wafer with an orientation closer to on-axis were also tried as an effort to further decrease the surface defect density. A larger area and a flatter monolayer graphene sheet was formed [21] on the substrate with a mis-orientation within 0.03°, as illustrated by the LEEM image in Fig. 6 (a) which was collected at a FOV of 50 μm. A different fraction of domains compared to the first attempt (cf. Fig. 6(b) and Fig. 4(b)) was also detected. These domains, marked A-C in Fig. 6(b), were further investigated using μ-LEED. The μ-LEED images from the three domains are shown in Fig. 6(c) and

they all show 3-fold rotation symmetry but also that the image from domain A is rotated 120° relative to those from domains B and C. The symmetry and difference in these μ-LEED patterns we suggest originate from the underlying 6√3x6√3 R30° buffer layer and its interaction with the graphene layer.

Typical C1s and Si2p spectra collected from a homogeneous large-area single graphene layer sample at different photon energies are displayed in Fig. 7(a) and 7(b), respectively. It is quite interesting to note that the bulk SiC signal in the C1s spectrum collected at a photon energy of 330 eV is not possible to detect already after a single layer of graphene has formed (Fig. 7(a)) but that the bulk SiC signal in the Si2p spectrum collected at a photon energy of 140 eV in Fig. 7(b) on the contrary is very sharp and intense, although the electron escape depth of these core levels at the specified energies is similar. These observations are supported by PEEM measurements [18] made, which suggest that the extra sharp Si2p SiC bulk signal originates from Si atoms in the topmost SiC bi-layer. These Si atoms are located very close to the graphene layer, which has metallic properties. This affect the spectral shape and give better resolved spin-orbit split peaks compared to from a typical SiC surface.

The terrace width on the SiC surface after graphene growth was in Figs. 4-6 shown to depend on the substrate mis-orientation. Although the difference in the off- orientation angle was fairly small, we could observe quite clearly that the bigger off-angle produced smaller terrace widths. In order to further confirm this observation, graphene was grown at similar conditions on an 8° off-cut substrate. Surprisingly, this produced a ribbon like

structure of monolayer graphene, as illustrated by the LEEM image at a FOV of 6 µm in Fig. 8(a). Recorded electron reflectivity curves showed the dark stripes to correspond to monolayer graphene and the bright stripes to the carbon buffer layer. Graphene ribbons alternating with the buffer carbon layer were thus obtained on this substrate and the width of the ribbons was found to vary between ca. 30 and 200 nm. Ribbons with widths in this range have been demonstrated [24] to be semiconductors with a band gap inversely proportional to the width. A typical LEEM image from this sample at a field of view of 50 µm is shown in Fig. 8(b). The darker area is where the stripes/ribbons of monolayer graphene have formed while at the brighter areas a few layers of graphene have actually grown. The µ-LEED pattern recorded from the bright areas shows only the middle graphite spot, Fig. 8(c), which indicates the presence of four or more layers of graphene. The µ-LEED pattern from the darker area, Fig. 8(d), contains also the surrounding spots that represent contribution from the carbon buffer layer with and without the monolayer graphene ribbons on top.

The above results explain why preparation of graphene by high temperature decomposition of silicon carbide in an argon atmosphere presently is considered a champion route for obtaining uniform high quality wafer size graphene layer(s) for future electronic device applications. The results also indicate that off-cut substrates may be of potential interest for applications if the formation of ribbons and especially the width of the ribbons can be controlled by the off-cut angle.

3.2 *In situ* and semi *ex situ* growth

The earlier studies [13-16] of epitaxial graphene growth on SiC were concentrated on preparation *in situ* by high temperature heating. This yielded nonuniform graphene samples with small grains, as illustrated above in Fig. 1(b). The obvious question is then why the quality of *in situ* prepared graphene is not comparable with that obtained by *ex-situ* furnace growth. Is it due to an uneven heating of the SiC substrate, the growth temperature or the base pressure during the heating/decomposition of SiC? Below we try to elucidate this by results of *in-situ* and semi *ex-situ* growth experiments on substrates cut from the same wafer as used to obtain the *ex-situ* results shown in Figs. 4, 5(a) and 5(b) above. The LEEM image in Fig. 9(a) is from a sample prepared *in situ* (i.e. ~10^{-9} torr) at a temperature of 1275°C by direct current heating and for which the temperature gradient across the surface was measured to be ≤ ±10°C, using a pyrometer. Only a first layer of graphene has started to develop on this sample, as indicated by the darker stripes/spots covering about half the surface area. Although this sample may appear more homogeneous than the one in Fig. 1(b) the stripes/flakes of graphene are much smaller than on the *ex-situ* prepared samples. One may think that by heating a bit longer time the stripes/flakes may grow and coalesce and make a large homogeneous graphene layer like on the *ex situ* prepared. Therefore another sample was prepared *in situ* at the same temperature but for a longer time and the result is illustrated in Fig. 9(b). The bright areas now show that the first layer of graphene is fully developed while the darker stripes indicate that a second layer has started to develop. Thus, the longer heating time had no effect on the size of the stripes/flakes and uniformity of the graphene sample. A LEED image collected from this sample, at an electron kinetic energy of 109 eV, is shown in Fig. 9(c). An interesting observation on these *in situ* prepared samples is that the width of the

elongated graphene stripes/flakes is essentially the same as the average terrace width on the clean substrate surface [18] before growth. This is a crucial discrepancy between the *in situ* and *ex situ* prepared samples that have to result from the different growth conditions playing an important role to control the size of the graphene flakes and layers. A higher growth temperature and a background ambient gas pressure, appear to be the main/key factors to control the quality of the graphene prepared. When increasing the growth temperature to ca. 1450°C and the background base pressure to about $1x10^{-3}$ torr, by introducing pure argon gas, the quality of the graphene sheet is improved as shown by the LEEM image in Fig. 9(d). This growth we label "semi- *ex situ*" since the background ambient gas pressure is lower than atmospheric pressure. The average size of the stripes/flakes formed is seen to be larger than for the *in situ* prepared samples. The electron reflectivity curves recorded from this semi- *ex situ* sample showed, however, the main bright areas to consist of three layers of graphene and the dark stripes to correspond to four layers. The improvement in quality is here the important point since it indicates that it appears possible to obtain fairly high quality graphene layers by direct current heating of SiC substrates in an ambient gas pressure. Further experiments varying the growth temperature and the ambient gas pressure are underway, since they hopefully can provide a simple and fast way for the preparation of fairly homogeneous graphene layers on SiC.

The above *in situ* and semi *ex situ* results indicate the reasons why graphene of much better quality is achieved by the *ex situ* growth method described in the previous section. In an earlier study [16] of graphene formation on SiC(0001) upon heating *in situ*,

collected LEEM and AFM data showed that the surface was rough when graphene formed. The steps were no longer straight and deep pits were observed. Pit formation was traced to the stability of the $6\sqrt{3}x6\sqrt{3}$ R30° buffer layer and the existence of gaps in the buffer layer coverage on each terrace. Rapid nucleation of the buffer layer was suggested to minimize the existence of gaps and to inhibit pit formation. It was concluded that the growth of smooth flat graphene films required heating at temperatures well above 1200°C, where however multiple layers of graphene would grow [13] when heating *in situ*. Our *ex situ* samples were prepared at a temperature of 2000°C in an argon ambient of one atmosphere and produced large domains of flat smooth graphene films. When taking a closer look at Figs. 4 and 5 one clearly see steps and terraces and that the average terrace width has changed quite dramatically compared to the terrace width on the *in situ* prepared samples (and the substrate), see Figs. 9(a) and (b). This indicates that the surface morphology is drastically changed after the *ex situ* growth, and this is suggested to be due to step bunching of the substrate. Much larger terraces have developed and a single layer of graphene has formed on these terraces. The heating temperature determines the kinetics of the elements involved. The surface mobility of carbon and the nucleation rate of the buffer layer are expected to increase considerably when raising the annealing temperature from 1200 to 2000°C. The sublimation rate of silicon, leaving carbon behind, should also increase with temperature. However, a surrounding ambient of Ar, instead of vacuum, is commonly used in sublimation growth experiments to suppress a too fast sublimation rate and provide a smooth decomposition of the SiC. In this particular case it results in both desirable growth and morphology changes, the formation of larger terraces with single layer graphene films on top. The *ex situ* samples

were heat treated in a designed arrangement to minimize the temperature gradient while the *in situ* sample was heated by running current through it, which creates a thermal gradient in the surface region. Although homogenous sample heating may be of importance for obtaining graphene layers of the highest quality, the results of ours [18, 21] and other groups [19, 20, 23] have proved that the use of a considerably higher growth temperature in combination with a background ambient gas pressure are the key factors for obtaining large homogenous layers of graphene. More information on the operational conditions elaborated in our growth experiments can be found in [25].

4 Atomic scale studies of homogeneous monolayer graphene

STM studies of graphene on SiC have to a large extent focused on the determination of differences between monolayer and bi-layer graphene [26-31]. This is, however, not the most straightforward way for a thickness determination [27, 29]. Mallet *et al.* [27] claimed that monolayer graphene shows hexagonal rings with six protrusions (honeycomb), while bi-layer graphene shows only three protrusions (hexagonal or the three for six arrangement) similar to graphite. The latter was suggested to be due to AB stacking of the layers. However, P. Lauffer *et al.* [29] unexpectedly observed areas of bi-layer graphene where the image did not show the expected triangular array of protrusion but rather resembled the monolayer case. Recently, Hibino *et al*. [31] also studied epitaxial bi-layer graphene using dark-field LEEM, dynamic LEED I-V and STM. Their results showed that bi-layer graphene consists of two types of domains with AB and AC stacking and their STM results showed presence of both the honeycomb and the three for

six patterns. These observations agree well with our recent findings in STM studies of homogeneous large area monolayer graphene [21] samples, as described and discussed below.

Large scale STM images of furnace-grown single layer graphene on respectively the 0.03°- and 0.25°-SiC(0001) substrates are shown in Fig.10 (a) and (b). Line profiles extracted along the dashed lines A and B in these figures are displayed in Fig. 10(c). They show step heights of ca. 10-15 Å, and an average terrace width of ~6 μm, on the 0.03°-SiC substrate and step heights of ca. 40-50 Å, and an average terrace width of ~2 μm, on the 0.25°-SiC substrate. It is important to point out that on the 0.03°-SiC substrate, the graphene sheet was found to grow continuously over the steps edges and over an area larger than 50 μm^2. It is clearly seen in Fig. 11(a) that the honeycomb network of carbon atoms grows continuously over a step edge with the same registry from the upper terrace to the bottom terrace. At the edge, the graphene sheet is found to roll up over the edge before folding down to the lower terrace, as the line profile across the step in Fig. 11(b) shows (red arrow). This effect has been observed earlier using HR-TEM [30]. When the step height was larger, an atomic resolution could no longer be achieved close to the edge. This is probably because then the electrons do not tunnel only at the end of the tip but also from other positions. Therefore the continuation of the graphene layer over the higher step edges occurring on the 0.25°-SiC substrate could not be determined in this experiment. We can therefore only conclude that these graphene sheets on the 0.25°-substrate have an average width of about 2 μm and a length of >25 μm. Atomically resolved images of the graphene sheet on the 0.03°- SiC substrate are shown in Fig.

12(a)-(c). The long range periodicity of charge densities from the underlying 6√3x6√3 R30° buffer layer is illustrated over an area of 40 x 40 nm^2 in Fig. 12(a). The honeycomb network from single layer graphene is resolved at a tip bias of -0.5 V, as shown in Fig. 12(b) and (c). The line profile (Fig. 12(d)) along the AA´ direction in Fig. 12(b) shows that the graphene sheet follows the corrugation of the buffer layer, with an amplitude of about 1.3 Å. It also shows the distance between the centers of the hexagonal rings to be about 0.25 nm, which Fig. 12(c) also illustrates. This agrees well with the typical value of the hexagonal graphene ring (0.246 nm). Surprisingly, the STM image in Fig. 12(c), which is recorded from the same area as Fig. 12(a) and (b), shows both a honeycomb-like network and a three-for-six arrangement. The honeycomb-like network is found mainly at the protrusions of the underlying buffer layer (bright areas) but, interestingly, the three-for-six arrangement is observed (red arrow) in the valleys. Since only one monolayer of graphene was observed in LEEM over a large area (>50 μm^2), the three-for-six arrangement observed here cannot represent the 2–3 ML of graphene as claimed earlier [26, 27]. Instead we suggest that the three-for-six arrangement represents 1 ML graphene with the stacking type that does not match well with the carbon atoms in the buffer layer (similar to the AB type of bi-layer graphene [14]). We suggest the honeycomb-like arrangement around the protrusions to represent 1 ML graphene with a stacking that matches well with the carbon atoms in the buffer layer (similar to the AA type [14]). Essentially identical STM results were obtained from monolayer graphene prepared on the 0.25°-SiC substrate. These findings [21, 31] support the suggestion of P. Lauffer *et al.* [29] that the identification of the number of graphene layers based solely on the appearance of the STM image, i.e. honeycomb or three for six arrangements, is

inadequate. They instead proposed the use of the thickness dependence of the interface-induced roughness of the outermost graphene layer to determine the number of layers present. However this method may not be applicable if the buffer layer can be eliminated, as discussed in the next section.

5 Buffer layer free interface and hydrogen interactions

It is well known [7, 8, 11-12] that the first carbon layer grown on the SiC(0001) substrate forms strong covalent bonds with the SiC substrate and has no graphitic electronic properties. This layer therefore acts as a buffer layer and allows the next carbon layer, i.e. first graphene layer, to behave electronically like an isolated graphene sheet. Reported DFT calculations [7] show that the buffer layer exhibits a large band gap and a Fermi level pinned by a state having a small dispersion and related to the dangling bonds in between the bulk SiC and this buffer layer. The existence of this buffer layer is regarded as a major obstacle for the development of future electronic devices from graphene on SiC(0001), because it may affect the transport properties.

It was recently reported [32-33] that exposures to a cold hydrogen plasma induced changes in the electronic properties of graphene that provided evidence that graphane could be synthesized. The hydrogen removed the conducting π-bands and opened up an energy gap. It was also recently reported that single layer graphene undergoes a metal-insulator transition already at a small coverage of atomic hydrogen and that the resistance then increases by about four orders of magnitude at room temperature [34]. However,

there are no reports that the hydrogen can improve the interface properties of epitaxial graphene grown on SiC substrates. Below we present and discuss our recent finding [22] that the carbon buffer layer underneath the graphene layer is affected after exposures to ionized or atomic hydrogen, and that it actually can be eliminated.

First we investigated the effects of hydrogen plasma exposures to graphene samples with a thickness of about one monolayer on SiC(0001). The samples were kept at room temperature and exposed for 10 min. to a hydrogen plasma at a pressure of $6x10^{-5}$ mbar. The C1s core level spectra collected, using a photon energy of 450 eV, before and after hydrogenation and after subsequent anneals at 600 and 950°C are displayed in Fig. 13. The spectra comprise of the same components as illustrated in Fig. 3. The hydrogen plasma exposure is seen to shift all components by about 0.4 eV towards lower binding energy but, more importantly, to significantly reduce the buffer layer component. The extracted G/SiC peak intensity ratio has increased by about a factor of two, which indicates the presence of about twice as much graphene as before the hydrogen plasma exposure. After annealing at 950°C the extracted B/SiC peak intensity ratio is almost back to the value before the exposure, but the spectral features are somewhat broader. Normal emission valence band spectra collected using a photon energy of 33 eV and under the same conditions as the four C1s spectra are shown in Fig. 14. The valence band spectrum is seen to contain two main components located at about 5 eV and 8.5 eV below the Fermi level and they originate respectively from a σ and π energy band. The σ component, which represents the in plane sp^2 bonding, is observed to decrease in intensity and broaden after the hydrogen plasma exposure but to regain strength after the

subsequent heating up to 950 °C. We suggest this to indicate that C-C sp^2 bonds are broken, i.e. disorder is induced, by the hydrogen plasma exposure but that they are partly re-established after heating to 950 °C. The π component is however shifted towards the Fermi level. This is interpreted to indicate a change in the surrounding of the carbon atoms in surface layers induced by the hydrogenation. These changes observed in the C1s and valence band spectra suggest that the hydrogen ions/atoms actually penetrate below the carbon buffer layer and produce a new and different interface to the SiC substrate.

We therefore later investigated if exposures to atomic hydrogen would give similar or different effects. These experiments we could do in the LEEM where atomic hydrogen was decomposed from H_2 gas passed through a tungsten capillary heated to about 2000 °C. The exposures in this case were performed at a pressure of about 10^{-7} mbar. The quality and thickness of the graphene layer grown on the SiC(0001) substrate was checked by LEEM and μ-LEED. The thickness was determined to be one single layer of graphene on most parts of the surface area. For navigation purposes we below however select to show an area, with a field of view of 50 μm, which partially contains two layers of graphene. The reason for this is that we then can determine that data is collected from exactly the same area before and after hydrogenation. The LEEM image collected before hydrogenation is shown in Fig. 15(a). The selected area (blue square) is confirmed to represent one layer of graphene by the recorded electron reflectivity curve shown in Fig. 15 (f) (bottom blue curve). Since it shows a single dip/minimum this area represents a monolayer of graphene. The bright area in Fig. 15(a) thus represents one layer of graphene while the darker areas/islands were determined to represent two layers of

graphene. The μ-LEED image, in Fig. 15(b), recorded from the same selected blue area show the local atomic order. The diffraction spot in the middle originates from the graphene layer while the six spots around it are contributions [12] from the ordered 6√3x6√3 R30° buffer layer underneath the graphene.

The LEEM picture in Fig. 15(c) was recorded after exposure to atomic hydrogen. Interestingly, this image of the graphene surface looks essentially identical as before the hydrogenation. None of the darker areas/islands have been removed or even changed shape. Surprisingly though the electron reflectivity curve collected from the same area (red square) now shows two dips/minima, as displayed by the middle red curve in Fig. 15(f). The two dips in the electron reflectivity curve characterize two layers of graphene on the SiC(0001) surface. Moreover, when checking the diffraction pattern from the same selected area, only one intense spot in the middle is detected. This is a contribution from graphene only so no sign of an ordered 6√3x6√3 R30° buffer layer remains after the atomic hydrogen exposure. The buffer layer appears to have been transformed to a graphene layer. It is worth pointing out that the bright surface area now contains two well ordered graphene layers since sharp LEEM images and sharp diffraction minima in recorded electron reflectivity curves as well as intense μ-LEED pattern were still obtained. The electron reflectivity curve from the darker areas now exhibited three dips instead of the two before hydrogenation. However, the minima in the curves from the graphene without the carbon buffer layer are slightly shifted compared to when the buffer layer is present, cf. Fig. 2(b). This we interpret to show the importance of the buffer layer in the overall electron reflection.

The new phase created by atomic hydrogen exposure was found to be stable and inert from room temperature up to a temperature of about 800°C, and even after storage in the open atmospheric for more than a month. After annealing this phase at a temperature of ca. 950°C for a few minutes the electron reflectivity curve collected from the same area again shows only one dip, as shown by the upper green curve in Fig. 15(f). Thus the bright surface area then again represents monolayer graphene. Interestingly, the diffraction pattern from the selected area again shows a contribution from the ordered buffer layer, as displayed by the re-appearance of the six spots surrounding the middle graphene spot in Fig. 15(e). The data presented in Fig. 15 show that the process is reversible, hydrogenation transforms the buffer layer into a graphene layer and dehydrogenation by annealing transforms this layer back into the buffer layer.

The ARPES results obtained from this sample also showed this to be the case. Before hydrogenation the monolayer graphene sample showed a single π-band and a linear dispersion across the K point, as illustrated in Fig. 16(a). After hydrogenation two π-bands are clearly seen around the K point, Fig. 16(b), representing bi-layer graphene. Of particular interest is that this samples was left in air for about two months and the intense and well defined π-bands were obtained already from the as introduced sample. The LEED pattern collected from the hydrogenated sample showed only the graphene spots, as illustrated in Fig. 16(d). After heating the hydrogenated sample to about 780°C, for a few minutes, the two π-bands start to vanish and gradually transform back into a single band, as seen in Fig. 16(c). The LEED pattern observed after the sample had been heated

to ca. 1000 °C is shown in Fig. 16(e), and the buffer layer spots are then clearly visible again.

From these findings we suggest a model for this reversible hydrogenation mechanism that is displayed in Fig. 17. A monolayer graphene grown on a SiC(0001) substrate includes the well known strongly bound and ordered buffer layer at the interface, as illustrated in Fig. 17(a). Upon hydrogenation, we suggest that hydrogen atoms go through the graphene sheet [22] and the buffer layer and then bond to the Si atoms at the SiC- buffer layer interface, i.e. they break the C-Si bonds there and passivate the Si dangling bonds created. This results in a hydrogen intercalation layer in between the SiC substrate and the two carbon layers. This means that the buffer layer is lifted up and no longer strongly bond to the SiC substrate so the buffer layer is actually transformed into a second graphene layer, as illustrated in Fig.17(b). The model explains the observations of two dips/minima in the electron reflectivity curves, the elimination of the six spots in the μ-LEED pattern characteristic of the strongly bound buffer layer and the two π-bands visible around the K point. The suggestion of hydrogen atom passivation of Si atom dangling bonds at the SiC substrate interface is supported by the observation of a shift of 0.4 eV in the C1s core level spectrum towards lower binding energy upon hydrogenation. This shift agrees well with the earlier determined value upon hydrogen passivation of hexagonal SiC surfaces [35].

It is worth mentioning that this bi-layer graphene prepared by hydrogen intercalation is expected to be smoother, show a smaller corrugation, than with the underlying buffer

layer. However to confirm if this is the case STM investigations of the interface-induced roughness of the outermost graphene layer need to be made.

Summary

A successful *ex situ* method of preparing large and uniform monolayer and bi-layer graphene sheet(s) has been reviewed. Included are also comparisons of different substrate orientations and different growth techniques as well as different guidelines for determining the number of layers of graphene grown. The morphology of the graphene film was shown to be different on substrates having mis-orientations of 0.03° and 0.25°, respectively, from on-axis. On the former, a continuous graphene sheet, covering also the < 15 Å high steps, and with a size larger than 50 μm^2 is shown to form. On the latter, higher steps, i.e. more pronounced step bunching, and smaller terrace widths (~2 μm) are revealed, and the graphene layer on the terraces shows predominantly one type of domain. Also 8° off-cut substrates was utilized, and on these the graphene formed long ribbons/stripes alternating with the carbon buffer layer on large parts of the substrate surface. On *in situ* samples prepared at a temperature ~1300°C smaller flakes/stripes and nonuniform graphene films were shown to form. When utilizing a higher growth temperature and a background ambient gas pressure, the so-called semi *ex situ* method, the size of the flakes was shown to become bigger. An explanation why the *ex situ* growth method provide superior quality of the graphene films formed has been given.

Collected LEEM, μ-LEED and ARPES data after atomic hydrogen exposures demonstrate unambiguously a transformation from monolayer graphene plus carbon buffer layer to bi-layer graphene with no carbon buffer layer. A model supporting these findings has been suggested. This is novel since no one earlier has reported the preparation of either homogenous large area bi-layer graphene or bi-layer graphene without the carbon buffer (interface) layer on SiC(0001). These findings are of fundamental interest and may also open up possibilities and opportunities for graphene-SiC based electronic devices as well as hydrogen storage.

Acknowledgements

Authors would like to acknowledge Dr. Tihomir Iakimov for the *ex situ* growth of graphene on SiC(0001) substrates. Support from the Swedish National Energy Administration is gratefully acknowledged.

References

[1] Berger C, Song Z M, Li T B, Li X B, Ogbazghi A Y, Feng R, Dai Z T, Marchenkov A N, Conrad E H, First P N and de Heer W A 2004 *Journ. Phys. Chem. B* **108** 19912

[2] Novoselov K S, Geim A K, Morozov S V, Jiang D, Katsnelson M I, Grigorieva I V, Dubonos S V and Firsov A A 2005 *Nature* **438** 197

[3] Novoselov K S, Jiang D, Schedin F, Booth T J, Khotkevich V V, Morozov S V and Geim A K 2005 *Proc. Natl Acad. Sci. USA* **102** 10451

[4] Geim A K and Novoselov K S 2007 *Nature. Mater.* **6** 183

[5] Geim A K 2009 *Science* **324** 1530 and *ref. therein.*

[6] Ohta T, Bostwick A, McChesney J L, Seyller Th, Horn K and Rotenberg E 2007 *Phys. Rev. Lett.* **98** 206802

[7] Berger C, Wu X, First P N, Conrad E H, Li X, Sprinkle M, Hass J, Varchon F, Magaud L, Sadowski M L, Potemski M, Martinez G and de Heer W A 2008 *Adv. In Solid State Phys.* **47**, 145 and *ref therein*

[8] Bostwick A, Emtsev K V, Horn K, Huwald E, Ley L, McChesney J L, Ohta T, Riley J, Rotenberg E, Speck F and Seyller Th 2008 *Adv. In solid State Phys.* **47** 159

[9] de Heer W A *et al*. 2007 *Solid State Commun.* **143** 92

[10] Van Bommel A J, Crombeen J E and Van Tooren 1975 *Surf. Sci.* **48** 463

[11] Johansson L I, Owman F and Mårtensson P 1996 *Phys. Rev. B* **53** 13793

[12] Mårtensson P, Owman F and Johansson L I 1997 *Phys. Status Solidi (b)* **202**, 501 and *ref therein*

[13] Ohta T, El Gabaly F, Bostwick A, McChesney J L, Emtsev K V, Schmid A K, Seyller Th, Horn K and Rotenberg E 2008 *New. J. Phys.* **10** 023034

[14] Hass J, de Heer W A and Conrad E H 2008 *J. Phys.: Condens. Matter* **20** 323202

[15] Hibino H, Kagashima K, Maeda F, Nagase M, Kobayashi Y and Yamaguchi H 2008 *Phys Rev. B* **77** 075413

[16] Hannon J B and Tromp R M 2008 *Phys. Rev. B* **77** 241404

[17] Sprinkle M, Soukiassian P, de Heer W A, Berger C and Conrad E H 2009 *Phys. Status Solidi RRL* **3** A91

[18] Virojanadara C, Syväjarvi M, Yakimova R, Johansson L I, Zakharov A A and Balasubramanian T 2008 *Phys. Rev. B* **78** 245403

[19] Emtsev K V, Bostwick A, Horn K, Jobst J, Kellog G L, Ley L, McChesney J L, Ohta T, Reshanov S A, Röhrl J, Rotenberg E, Schmid A K, Waldemann D, Weber H B and Seyller Th 2009 *Nature Mater.* **8** 203

[20] Tromp R M and Hannon J B 2009 *Phys. Rev. Lett.* **102** 106104

[21] Virojanadara C, Yakimova R, Osiecki J R, Syväjärvi M, Uhrberg R I G, Johansson L I and Zakharov A A 2009 *Surf. Sci.* **603** L87

[22] Virojanadara C, Zakharov A A, Yakimova R and Johansson L I 2009 *Surf. Sci. Lett. Inpress*, doi:10.1016/j.susc.2009.11.011

[23] Borovikov V and Zangwill A 2009 *Phys. Rev. B* **80** 121406

[24] Wang X, Ouyang Y, Li X, Wang H, Guo J and Dai H 2008 *Phys. Rev. Lett.* **100**, 206803

[25] Yakimova R, Virojanadara C, Gogova D, Syväjärvi M, Siche D, Larsson K, and Johansson L I 2010 *Mater. Sci. Forum inpress*

[26] Brar V W, Zhang Y, Yayon Y, Bostwick A, Ohta T, McChesney J L, Horn K, Rotenberg E and Crommie M F 2007 *Appl. Phys. Lett.* **91** 122102

[27] Mallet P, Varchon F, Naud C, Magaud L, Berger C and Veuillen J –Y 2007 *Phys. Rev. B* **76** 041403

[28] Rutter G M, Crain J N, Guisinger N P, Li T, First P N, Stroscio J A 2007 *Science* **317** 219

[29] Lauffer P, Emtsev K V, Graupner R, Seyller Th, Ley L, Reshanov S A and Weber H B 2008 *Phys. Rev. B.* **77** 155426

[30] Liu Z, Suenaga K, Harris P J F and Iijima S 2009 *Phys. Rev. Lett.* **102** 015501

[31] Hibino H, Mizuno S, Kageshima H, Nagase M and Yamaguchi H 2009 *Phys. Rev. B* **80** 085406

[32] Elias D C, Nair R R, Mohiuddin T M G, Morozov S V, Blake P, Halsall M P, Ferrari A C, Boukhvalov D W, Katsnelson M I, Geim A K and Novoselov K S 2009 *Science* **323**, 610

[33] Savchenko A 2009 *Science* **323** 589

[34] Bostwick A, McChesney J L, Emtsev K V, Seyller Th, Horn K, Kevan S. D and Rotenberg E 2009 *Phys. Rev. Lett.* **103** 056404

[35] Sieber N, Mantel B F, Seyller Th, Ristein J, Ley L 2001 *Diamond and Related Materials* **10** 1291

Table 1.

Method	Thickness (ML)	G/SiC	B/SiC	G/B
μ-PES	**0.5**	**0.8**	**1.3**	**0.6**
	1	**3.0**	**1.4**	**2.1**
	3	**4.5**	**1.7**	**2.6**
PES	**0.5**	**1.8**	**2.3**	**0.7**
	1	**3.8**	**1.8**	**2.2**
	1-2	**4.7**	**1.6**	**2.9**

Table caption

Table1. The intensity ratio extracted from different components in the C1s spectra displayed in Fig. 3.

Figure captions

Fig. 1. Graphene prepared by two different methods. (a) mechanical exfoliation, the graphene flake visualized by atomic force microscopy [4]. (b) epitaxial growth on the SiC(0001) surface by high temperature annealing (1310°C) in vacuum, LEEM image at a FOV of 5 μm and recorded with an electron energy of 4.08 eV [13].

Fig. 2. (a) LEEM image from an area with different number of graphene layers formed. The FOV is 20 μm and the electron energy 4.2 eV. Inset are μ-LEED patterns collected at E= 53.3 eV from the four labeled areas. (b) Electron reflectivity spectra extracted from the four representative areas labeled (1)-(4) and corresponding to graphene of 1-4 ML thick, respectively.

Fig. 3. C1s spectra collected from graphene of different thicknesses using a photon energy of 450 eV, (a) μ-PES and (b) conventional PES. Peaks underneath show the components obtained when applying a fitting procedure. The 0.5 ML spectra were collected from an *in situ* prepared sample, while the other spectra were collected from *ex situ* prepared samples [18].

Fig. 4. (a) LEEM image of a single domain monolayer graphene sheet grown *ex situ* on SiC(0001); FOV is 20 μm and the electron energy is 4.4 eV. (b) LEEM image illustrating the existence of two domains of monolayer graphene, the three dark stripes represent two monolayers. The same voltage and 50 μm FOV is used in this case. (c) LEEM image of

an area containing a deep scratch; FOV is 50 μm and the electron energy is 0.1 eV. (d) A typical LEEM image from the 1st try of *ex situ* prepared samples showing that the layer coverage is one (bright) and two (dark), predominantly on this sample. The FOV is 50 μm and the electron energy 4.0 eV.

Fig. 5. (a) LEEM image of graphene grown on a 0.25°-SiC substrate, the FOV is 25 μm and energy 4.4 eV. (b) LEEM image from the same area recorded at an energy of 3.1 eV. The white stripes correspond to 2 ML thick graphene while the two sorts of gray areas represent two different domains of monolayer graphene. (c) LEEM image, by Emtsev et al [19], of graphene on 6H-SiC(0001) with a nominal thickness of 1.2 ML and grown by heating in Ar (p= 900 mbar, T = 1650°C); FOV is 15 μm and the energy 5.2 eV. The terraces are covered with monolayer graphene while bilayer and trilayer graphene has formed close to the step edges.

Fig. 6. LEEM images taken from monolayer graphene grown on a 0.03°-SiC substrate, the FOV is 50 μm and the energy 4.4 eV. (b) Image from same sample at a FOV of 25μm and energy of 2.1 eV. (c) μ-LEED images collected at E_{Kin} = 16 eV from the three labeled areas in (b) [21].

Fig. 7. Conventional PES of the (a) C1s and (b) Si2p core levels collected from an *ex situ* prepared homogeneous single graphene layer sample using different photon energies [18].

Fig. 8. LEEM images taken from graphene grown on an 8° off-cut SiC substrate. In (a) the field of view (FOV) is 6 μm and the electron energy 7.0 eV. The dark and bright stripes correspond respectively to monolayer graphene and zero layer graphene. (b) FOV is 50 μm and same electron energy. The white (arrow c) and dark (arrow d) areas correspond to thicker graphite layer and the stripes area displayed in the close-up LEEM image (a), respectively. μ-LEED images collected at E_{Kin} = 53 eV from the two areas labeled c) and d) in (b).

Fig. 9. (a) LEEM image from an *in situ* prepared sample recorded at an electron energy of 7.0 eV and a FOV of 20 μm. (b) LEEM image from an *in situ* prepared sample (same procedure but longer time), at a FOV of 15 μm and energy of 4.1 eV. LEED pattern recorded from the same sample at E_{Kin} = 109 eV and the Γ-M direction aligned horizontally. (d) LEEM image of the graphene formed after semi- *ex situ* growth, i.e. after heating at T = 1450°C in an Ar pressure of 10^{-3} torr; FOV is 15 μm and the energy 3.8 eV.

Fig. 10. Large scale STM images recorded from the (a) 0.03°-SiC substrate sample at 0.2nA and +0.5V) and (b) the 0.25°-SiC substrate sample at 0.1nA and +2.0V). Typical step heights and terrace widths are illustrated by the extracted line profiles in (c) [21].

Fig. 11. (a) Atomically resolved STM image of a graphene covered step on the 0.03°-SiC sample (0.2 nA, -0.2 V) and (b) a line profile across the step [21].

Fig. 12. STM images recorded from the same region at the size of (a) 40x40 nm^2, (b) 8x8 nm^2, (c) 2x2 nm^2 (0.2 nA, -0.5 V) and (d) a line profile extracted from image (b) [21].

Fig. 13. C 1s core level spectra collected at 450 eV photon energy from the *ex situ* prepared graphene SiC(0001) sample, before and after hydrogen plasma exposure and annealing at two different temperatures [22].

Fig. 14. Valence band spectra recorded at normal emission, at a photon energy of 33 eV, before and after hydrogenation and annealing at two different temperatures [22].

Fig. 15. (a) LEEM image recorded from monolayer graphene grown on SiC(0001). The FOV is 50 μm and the electron energy 1.2 eV. (b) μ-LEED image collected at E_{Kin} = 53 eV from within the selected blue square area. (c)-(d) LEEM and μ-LEED images recorded from the same areas after atomic hydrogen exposure. (e) μ-LEED pattern collected from the same selected area after annealing at 950°C. (f) electron reflectivity curves recorded from the selected square areas before (blue), after hydrogenation (red), and after annealing at 950°C (green) [22].

Fig. 16. The π band around the K point recorded from (a) monolayer graphene, (b) after hydrogenation and (c) after annealing at 780°C. (d)-(e) LEED patterns recorded after hydrogenation and after annealed to 1000°C, respectively; E_{Kin}= 80 eV and the sample is aligned with the Γ-K direction horizontally. (f) Schematic drawing of the 2D Brillouin zone of graphene.

Fig. 17. (a) A schematic structural model for monolayer graphene on the SiC(0001) substrate including a strongly bound ordered 6√3x6√3 R30° carbon buffer layer at the interface. (b) The structural model suggested for the new phase formed, having a hydrogen intercalated layer in between the SiC substrate and the initial 6√3x6√3 R30° buffer layer which now has become the a second graphene layer [22].

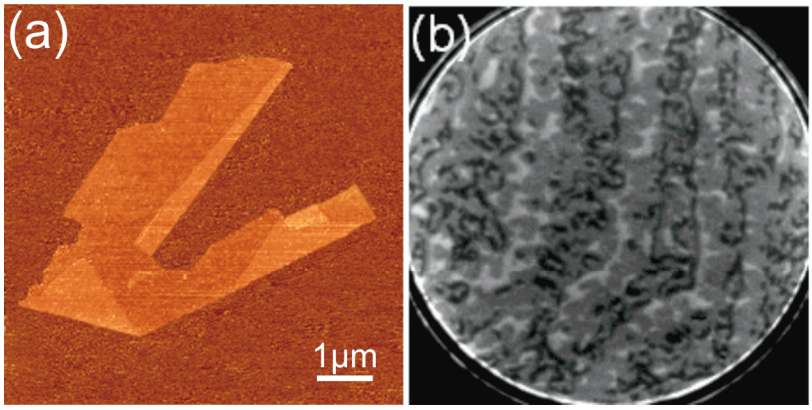

Fig. 1

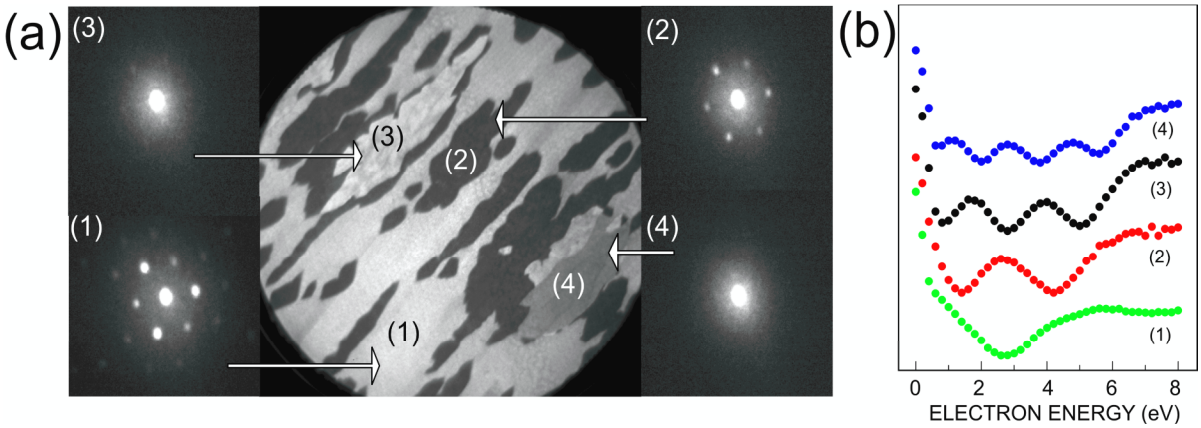

Fig. 2

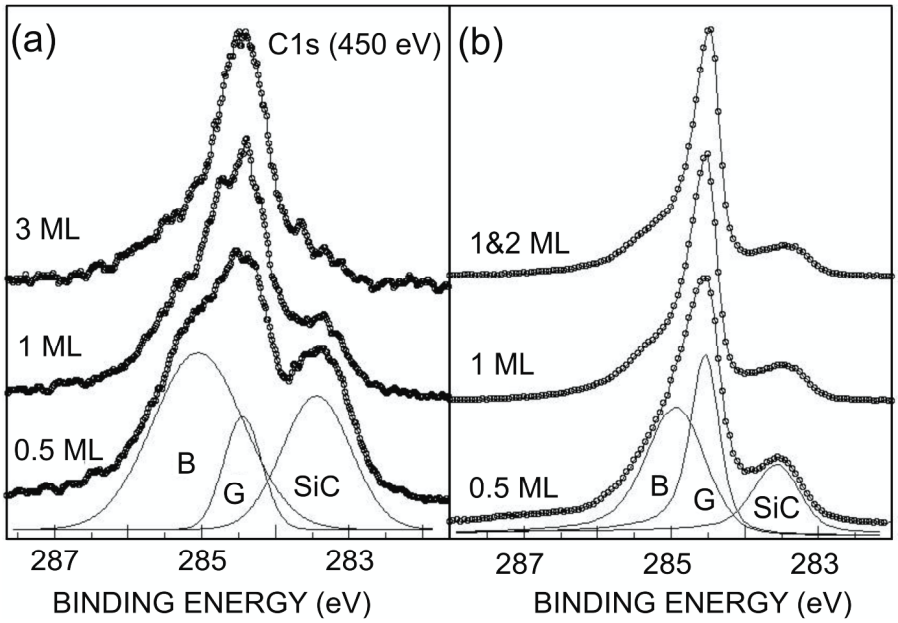
(a)
C1s (450 eV)
3 ML
1 ML
0.5 ML
B
G
SiC
287
285
283
BINDING ENERGY (eV)
(b)
1&2 ML
1 ML
0.5 ML
B
G
SiC
287
285
283
BINDING ENERGY (eV)

Fig.3

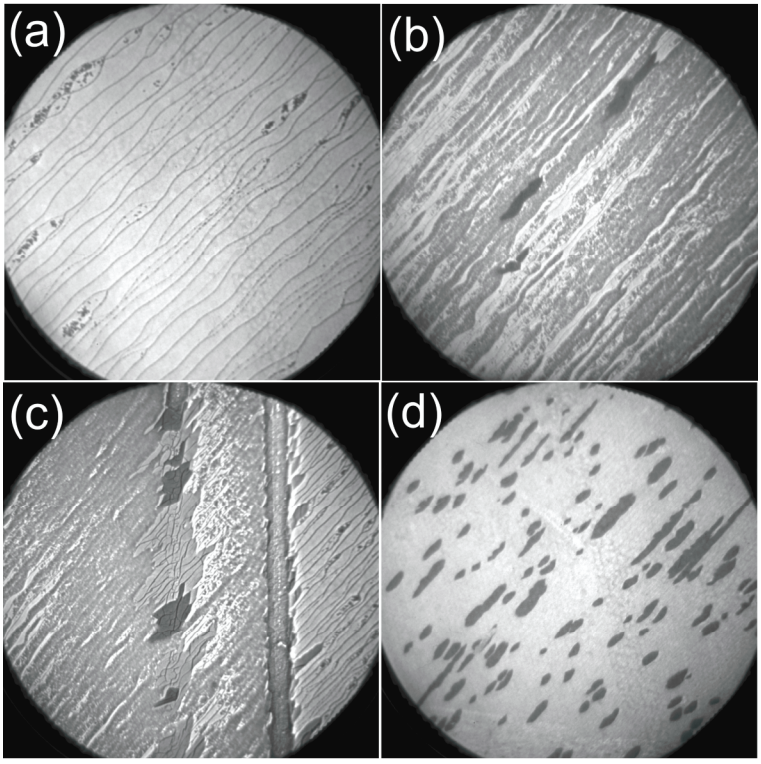
(a)
(b)
(c)
(d)

Fig. 4

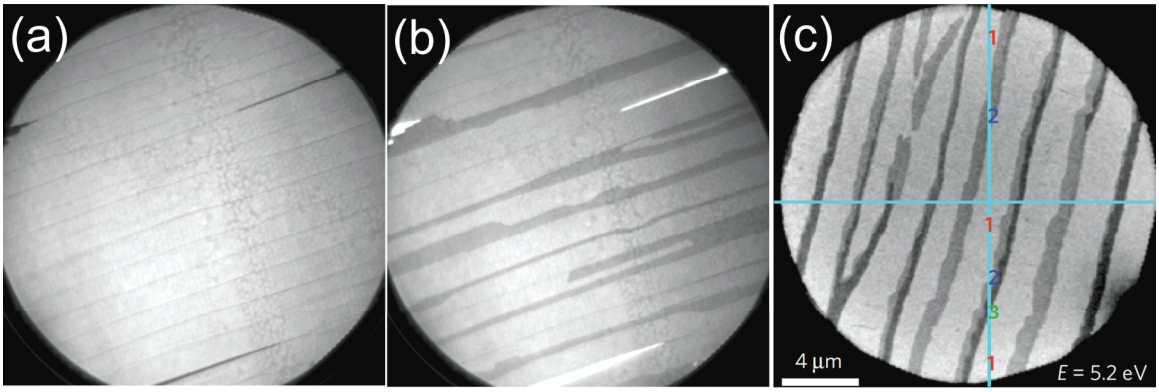

Fig. 5

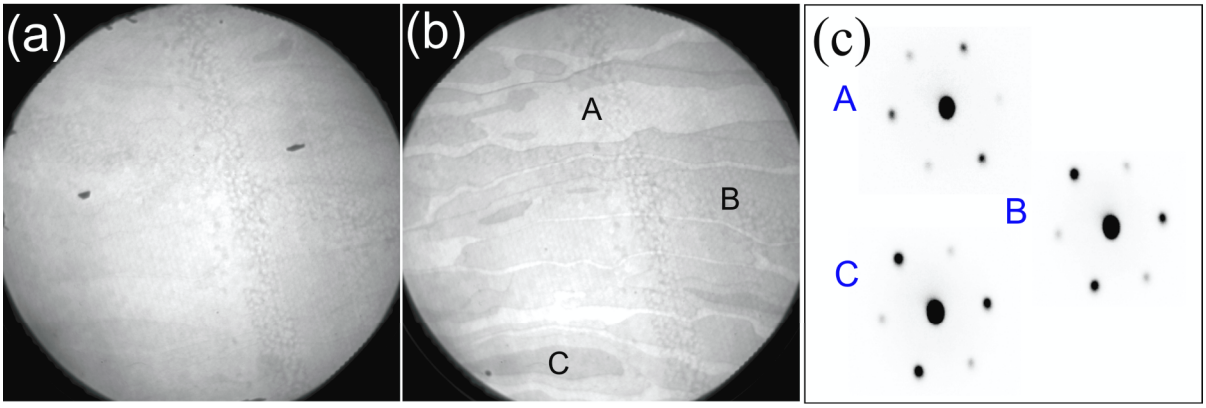

Fig. 6

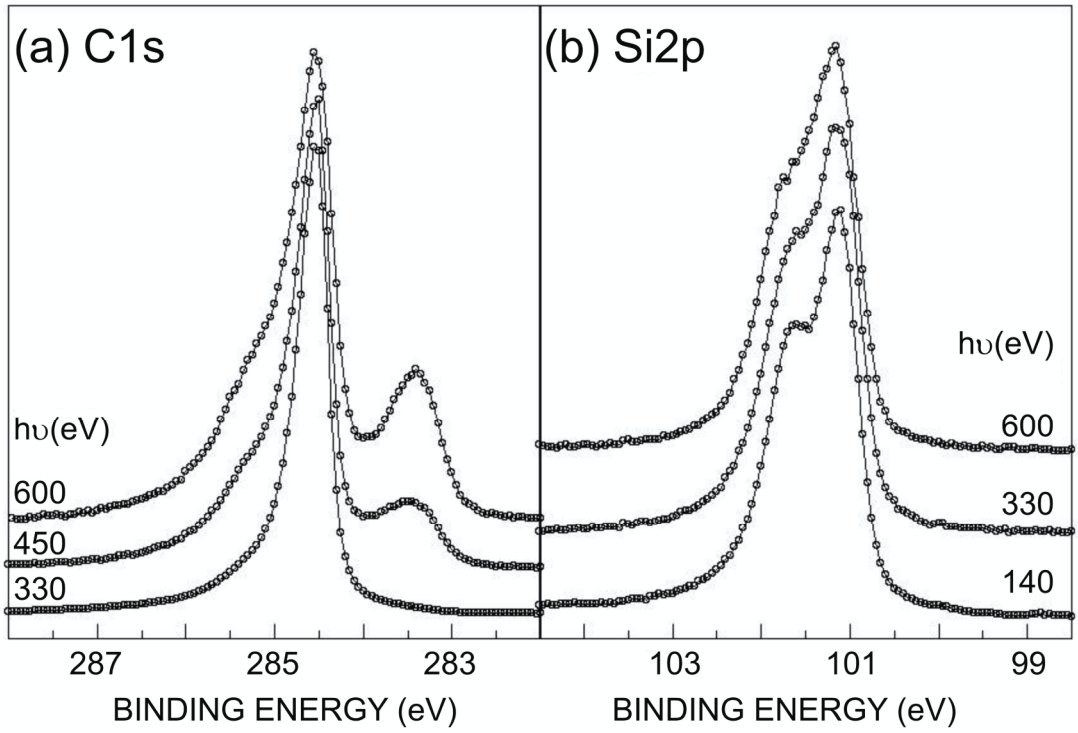
(a) C1s
(b) Si2p
hυ(eV)
600
450
330
hυ(eV)
600
330
140
287
285
283
103
101
99
BINDING ENERGY (eV)
BINDING ENERGY (eV)

Fig. 7

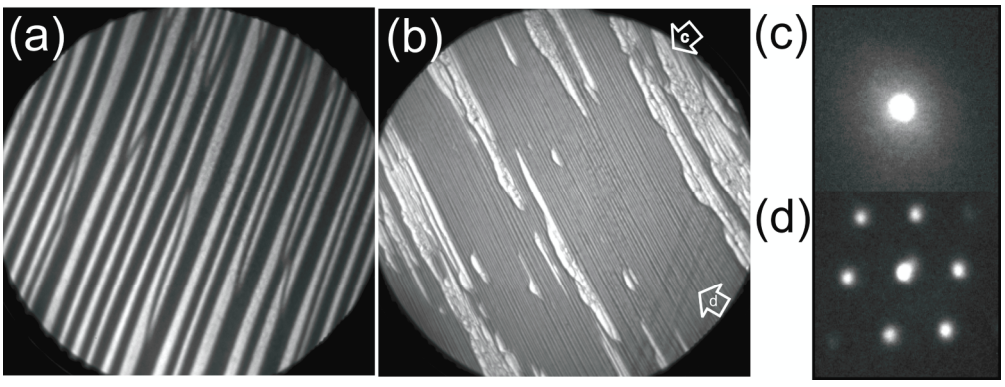
(a)
(b)
c
d
(c)
(d)

Fig. 8

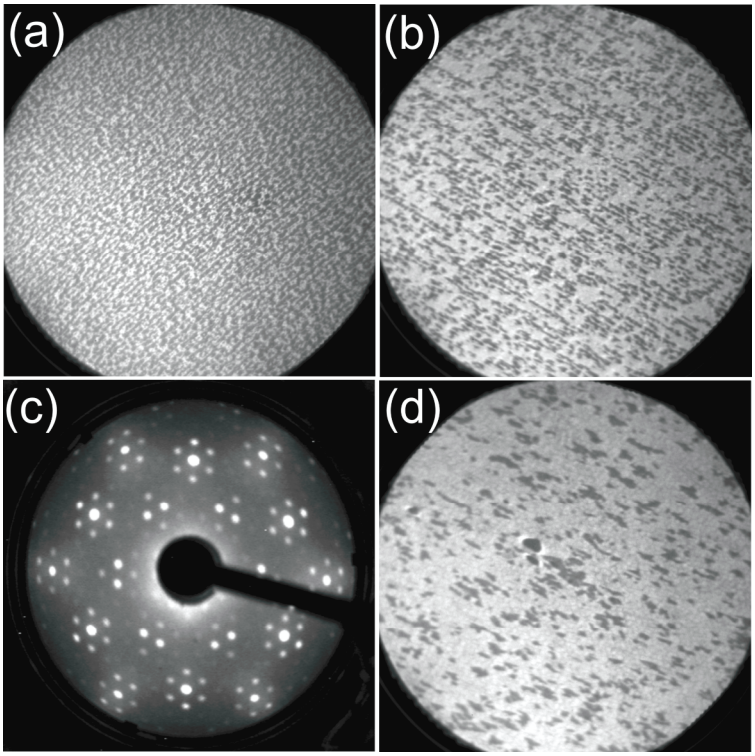

Fig. 9

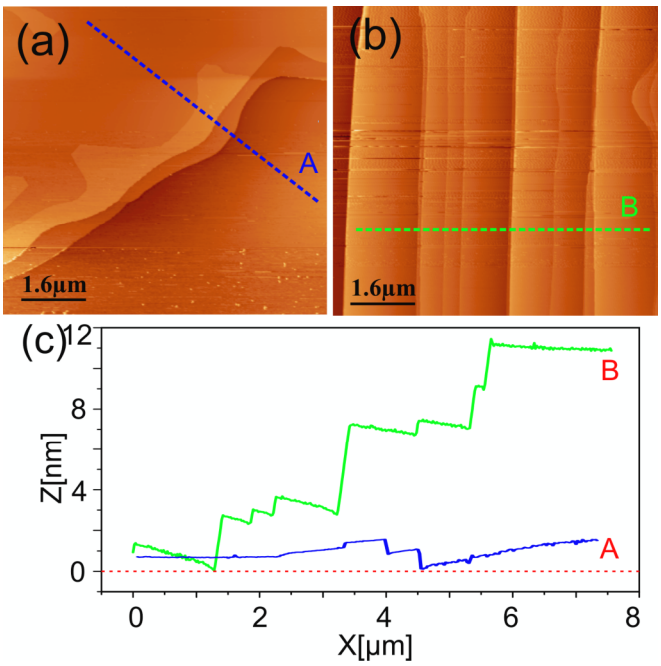

Fig. 10

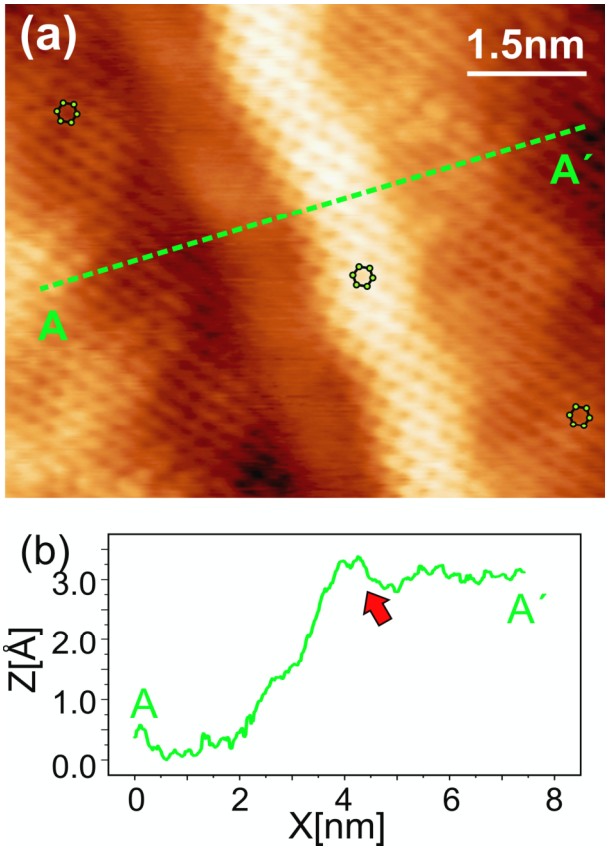
(a)
1.5nm
A´
A
(b)
3.0
2.0
1.0
0.0
Z[Å]
A´
A
0
2
4
6
8
X[nm]

Fig. 11

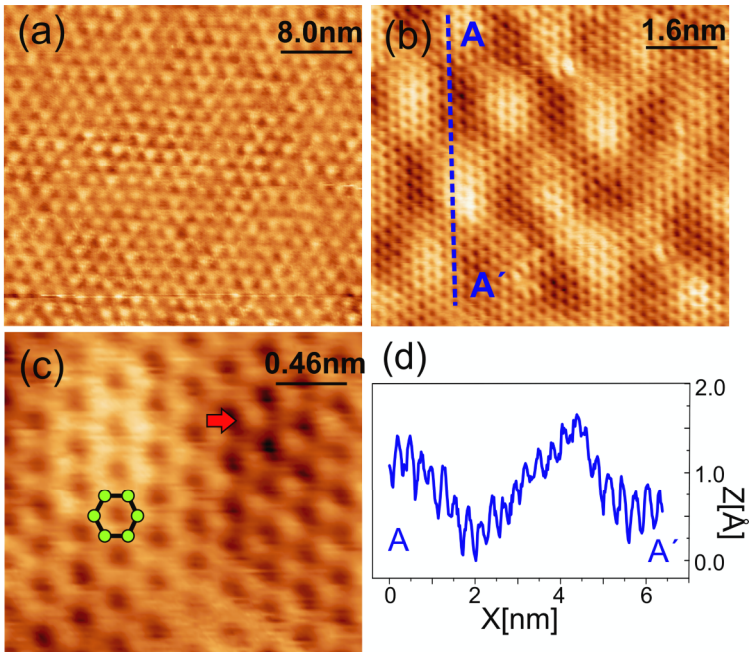
(a)
8.0nm
(b)
A
1.6nm
A´
(c)
0.46nm
(d)
2.0
1.0
0.0
Z[Å]
A
A´
0
2
4
6
X[nm]

Fig. 12

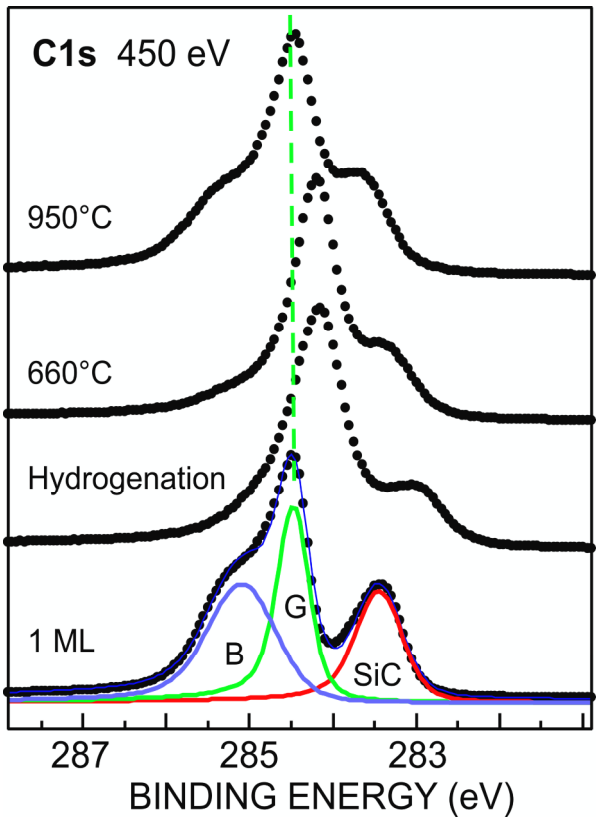
C1s 450 eV
950°C
660°C
Hydrogenation
1 ML
B
G
SiC
287
285
283
BINDING ENERGY (eV)

Fig. 13

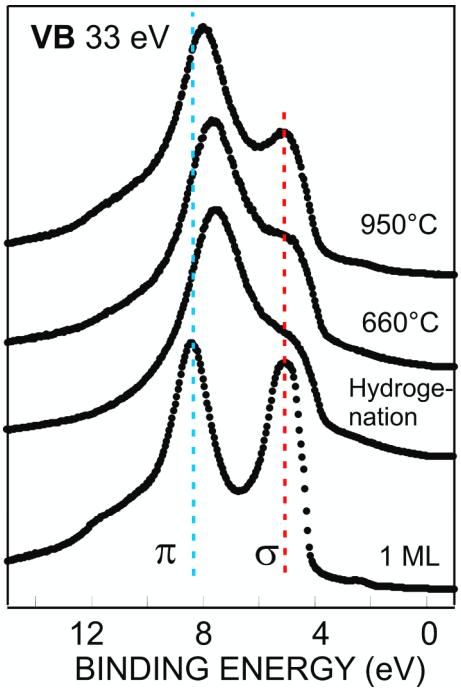
VB 33 eV
950°C
660°C
Hydroge-
nation
1 ML
π
σ
12
8
4
0
BINDING ENERGY (eV)

Fig. 14

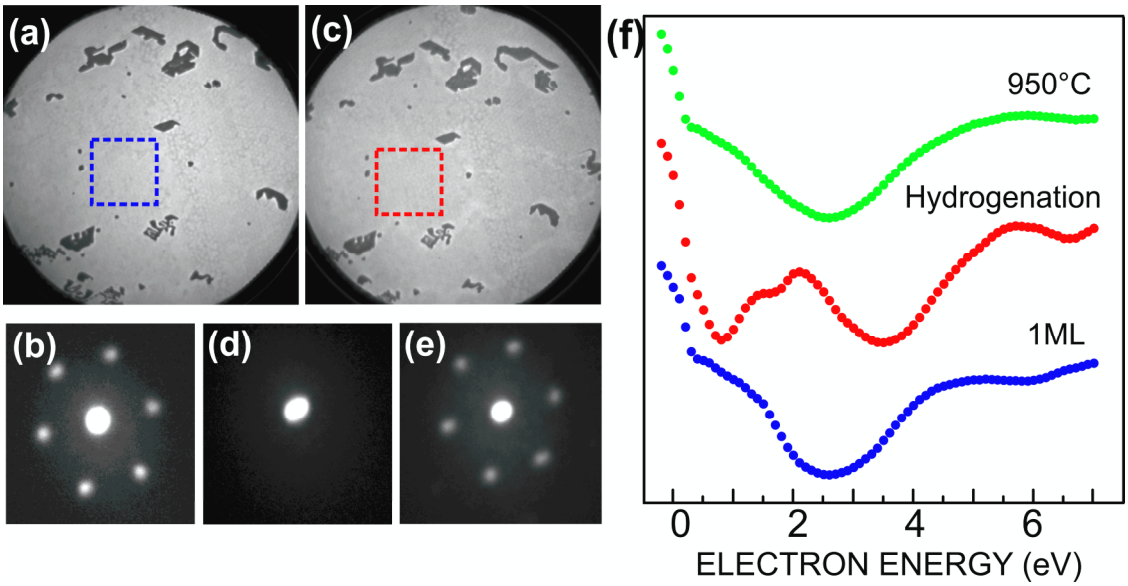
(a)
(c)
(b)
(d)
(e)
(f)
950°C
Hydrogenation
1ML
0
2
4
6
ELECTRON ENERGY (eV)

Fig. 15

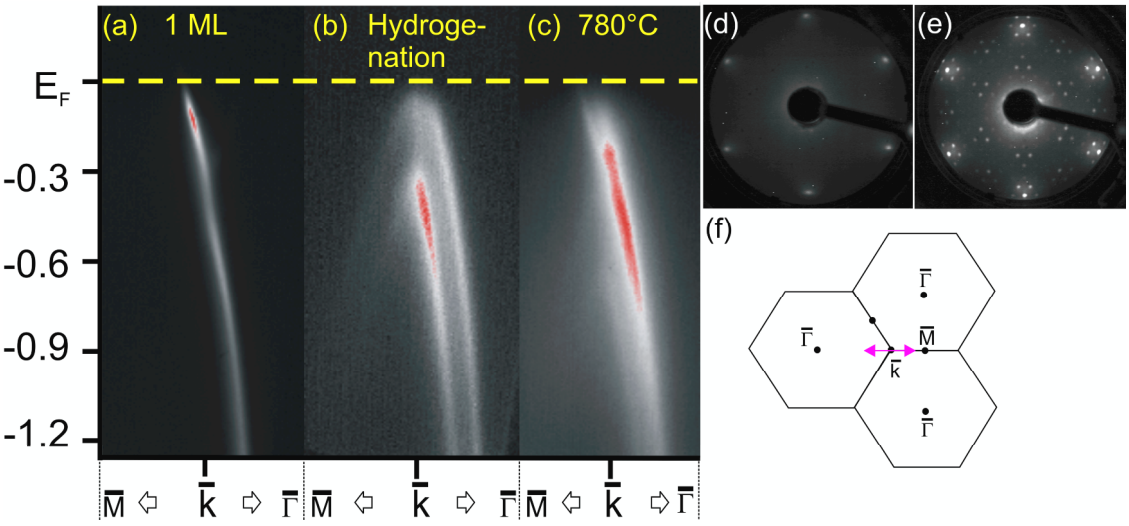
(a) 1 ML
(b) Hydroge-
nation
(c) 780°C
E_F
-0.3
-0.6
-0.9
-1.2
M̄ ⇦ k̄ ⇨ Γ̄
(d)
(e)
(f)
Γ̄
M̄
k̄

Fig. 16

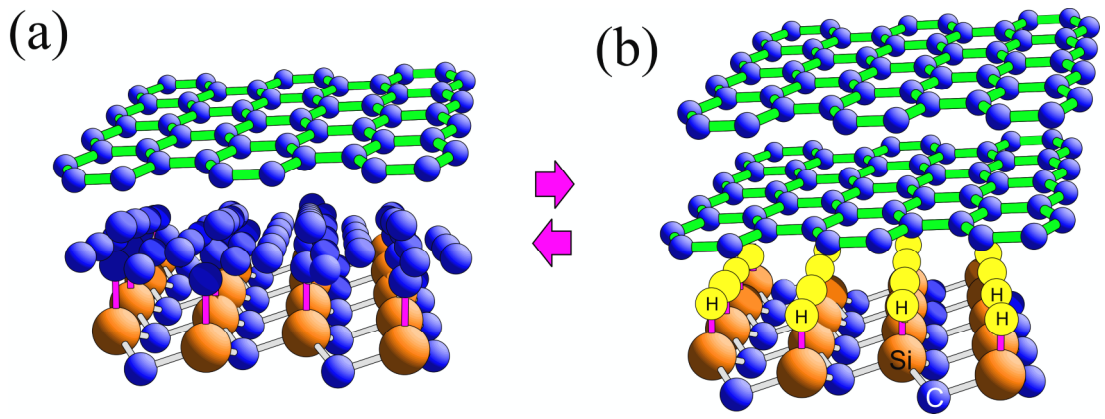

Fig. 17